Carbohydrate Polymers 102 (2014) 513–520

Contents lists available at ScienceDirect

Carbohydrate Polymers

journal homepage: www.elsevier.com/locate/carbpol

Designing slow water-releasing alginate nanoreserviors for sustained irrigation in scanty rainfall areas

Raineesh Sharma [a], Jaya Bajpai [a], A.K. Bajpai [a,*], Somen Acharya [b], R.B. Shrivastava [b], S.K. Shukla [c]

[a] Bose Memorial Research Laboratory, Department of Chemistry, Government Autonomous Science College, Jabalpur, M.P. 482001, India
[b] Defence Institute of High Altitude Research, Leh-Laddakh, J&K, India
[c] Central Water Commission, Ministry of Water Resources, Nagpur, MH, India

ARTICLE INFO

Article history:
Received 20 October 2013
Accepted 27 November 2013
Available online 6 December 2013

Keywords:
Nanoparticles
Alginate
Slow release
Deswelling
Agriculture

ABSTRACT

In this study, water absorbing Ca^{2+} ion cross-linked alginate nanoparticles were prepared and their water holding capacity was assessed. The prepared nanoparticles were characterized by Fourier transform infra red (FTIR) and X-ray diffraction (XRD) spectroscopy, field emission scanning electron microscopy (FESEM), and Zeta potential measurements to gain insights into their structural and morphological features and to see if the nanoparticles carried a charge over them. The swelling experiments were performed for different compositions of prepared nanoparticles at varied pH and temperatures. The capacity of the nanoparticles to retain imbibed water was evaluated by conducting deswelling studies of the pre-swollen nanoparticles. These particles were mixed with soil and soil-pot experiments were conducted. In order to assess the sustained water release potential of nanoparticles in agricultural fields, the seeds were planted in both native and nanoparticle-mixed soil pots, and moisture content of the soil was measured periodically and growth of the plants was observed.

1. Introduction

Nanotechnology, the science of working with the smallest possible particles, has raised hopes to overcome certain problems often encountered in agriculture. In agriculture, nanotechnology has already significantly impacted in areas like breeding of new crop varieties, development of new functional materials and smart delivery systems for agrochemicals such as herbicides, fertilizers, and pesticides, smart systems integration for food processing and packaging, and has affected other areas such as remediation of herbicide and pesticide residues from plants and soil and effluent water treatment (Mararu Carmen et al., 2003). In biomedical areas also the skills of nanotechnology have been successfully used for artificial implants (Wang et al., 2003), and enzyme immobilization (Betigeri & Neau, 2002). Applications of nanosystems also include controlled release technology, which is being intensively used in pharmaceuticals (Peppas, Bures, Leobandung, & Ichikawa, 2000) and agriculture (Bajpai & Giri, 2003). Controlled-release polymer matrix systems potentially offer numerous advantages over conventional applications (Sershen & West, 2002) and the principal advantage of these systems is that they require much less active agents to achieve desired results (Yeh, Kopekova, & Kopeek, 1994), thus making their use more economically viable than that of traditional methods.

In modern agricultural practice, many hydrophilic polymers are used to enhance both the nutritional and water status of plants. It has been reported that these hydrophilic polymers are capable of retaining water up to 500 times their initial weight (Buchholz, 1998) and can build up an additional water reservoir for the plant–soil system (Bouranis, Theodoropoulus, & Drossopoulus, 1995). Polysaccharides, such as chitosan, alginate, pectin, and cellulose are naturally occurring carbohydrate-based biopolymers. Apart from being non-toxic, they offer high water solubility, biocompatibility, and biodegradability (Philips & Williams, 2000). A significant feature of these biopolymers is the presence of high density functional groups (*e.g.*, amino groups in chitosan and carboxylic groups in pectin and alginate) that can be used for cross-linking to fabricate functional micro-gels. For example, alginate is known to form complexes with divalent ions such as Ca^{2+}, Ba^{2+}, and Sr^{2+} in aqueous solution. In addition, these polymers with moieties, such as the amino and carboxylic groups, are very sensitive to pH (Denuziere, Ferrier, & Domard, 1996; Kim, Yuk, & John, 1997; Pillay & Fassihi, 1999). The synthesis of microparticles from these biopolymers has long been the focus of intensive research in biomedicine, the pharmaceutical and cosmetics industries (George & Abraham, 2006), as well as agriculture (Oh,

* Corresponding author. Tel.: +91 0761 2320737; fax: +91 0761 2625514/5045219.
E-mail addresses: akbmrl@yahoo.co.in, akbajpailab@yahoo.co.in (A.K. Bajpai).

0144-8617/$ – see front matter © 2013 Elsevier Ltd. All rights reserved.
http://dx.doi.org/10.1016/j.carbpol.2013.11.059

Drumright, Siegwart, & Matyjaszewski, 2008). Alginate is a naturally occurring anionic polysaccharide commonly found in marine environments (Gombotz & Wee, 1998 and Davis, Llanes, Volesky, & Mucci, 2003). It is probably one of the most frequently studied hydrogel-forming biocompatible polymers. Structurally it is a linear copolymer composed of (1,4)-linked β-D-mannuronate and its C-5 epimer α-L-guluronate residues. It is insoluble in water but dissolves in some basic solutions by forming sodium salts due to its simple gelation with divalent cations such as Ca^{2+} (Gregor, Fenton, Brokenshire, Van Den Brink, & O'Sullivan, 1996).The presence of water in soil is essential for vegetation. In liquid form, water ensures the feeding of plants with nutritive elements that enable plants to achieve better growth rates. It is very important to exploit existing water sources by reducing water loss to ensure better living conditions for vegetation. Given the water-imbibing characteristics of superabsorbent polymer (SAP) materials, the possibilities for their application to alleviate certain agriculture problems have increasingly been investigated. SAPs are materials that absorb water and swell to many times their original size and weight. They are lightly cross-linked networks of hydrophilic polymer chains. These networks can swell in and hold a large amount of water while maintaining their internal structure (Buchholz & Graham, 1997; Zohuriaan-Mehr & Kourosh Kabiri, 2008). Commercially used water-absorbent polymeric materials are partially neutralized products of cross-linked polyacrylic acids or partially hydrolyzed products of starch-g-polyacrylonitrile and starch-g-polyacrylic acid copolymers. At present, their biodegradability is considered as an important prerequisite in this field because of renewed worldwide attention to environmental protection (Lentz, 2003). SAP hydrogels potentially influence soil permeability, density, structure, texture, evaporation, and the infiltration rates of water through soils. Moreover, these hydrogels can also reduce irrigation frequency and compaction tendencies, stop erosion and water runoff, and increase soil aeration and microbial activity (Abd EI-Rehirn, Hegazy, & Abd El-Mohdy, 2004).

Thus, the present study focuses on designing alginate-based nanocarriers and evaluating their slow water-releasing potential for possible agricultural applications in cold desert areas where rainfall is infrequent and water is scarce.

2. Experimental

2.1. Materials and methods

Sodium alginate was purchased from Research Lab, Pune, India, and used without further treatment. Calcium chloride (Dihydrate) obtained from Loba Chemie, Mumbai, India, was used as a cross-linking agent for alginate. Liquid paraffin oil (Marck, India) was used for an oil phase to prepare a microemulsion. Double-distilled water was used throughout the experiments. Sandy soil that was used for pot experiments was collected from the cold desert areas of Leh-Laddakh (India). A digital moisture meter was used to measure moisture content in the soil.

2.2. Preparation of the alginate nanoparticles

The calcium alginate nanoparticles were prepared by the emulsion cross-linking method. In brief, an aqueous phase was prepared by dissolving 1.0 g of sodium alginate in 30 mL of lukewarm distilled water while an oil phase was prepared using 10 mL of paraffin oil. These two solutions were mixed with a magnetic stirrer (capacity 5 MLH 300 rpm, Remi, India) for 30–40 min to form a stable emulsion. In the second step, 10 mL of cross-linker (0.5 mol/L calcium chloride) was added dropwise (1 mL min^{-1}) to the alginate emulsion while stirring it with a magnetic stirrer at a speed of 100 rpm. The cross-linking reaction was allowed to take place for 3 h at room temperature, and as a result, cross-linked nanoparticles of alginate were produced. The fine nanoparticles were formed which were allowed to stand for 24 h, then washed several times with toluene and acetone and finally dried under vacuum.

2.3. Characterization

2.3.1. FTIR spectral analysis

FTIR spectral analysis was carried out for structural characterization of the nanoparticles. The FTIR spectra of cross-linked nanoparticles were recorded in the range of 4000–400 cm^{-1} on a FTIR spectrophotometer (8400S, Shimadzu).

2.3.2. X-ray diffraction analysis

The X-ray diffraction studies of the nanoparticles were carried out on a Philips PW1820 powder diffractometer. The diffraction data were collected from 10° to 80°, 2θ values with a step-size of 0.02 and counting time of 2 s $step^{-1}$.

2.3.3. Surface charge (zeta potential) measurements

The sample was prepared by dispersing a known weight of nanoparticles in water that had a viscosity of 0.8878 cP and a dielectric constant of 78.3 as a dispersant. The dispersion was placed in a disposable zeta cell after which the surface charge of the nanoparticles was determined using a Zetasizer (Delsa TM Nano Z Instrument). A Zeta potential distribution curve was obtained between Zeta potential (mV) and intensity (kcps). The measurements were performed at 25 °C with a count rate of 2272.3 kcps.

2.3.4. Field emission scanning electron microscopy analysis

0.1 mL of alginate suspension was prepared in distilled water and Field Emission Scanning Electron Microscopy (FESEM) was performed using a Leo/Zeiss 1530 Field Emission Scanning Electron Microscope with an acceleration voltage of 5.0 kV.

2.3.5. Swelling experiments

A conventional gravimetric procedure (Barens & Hopfenberg, 1978; Saiyed et al., 2003) was used to monitor progress of the water sorption kinetics. The water sorption by the alginate nanoparticles was quantified by placing them in water and determining their weight periodically with a digital balance (APX-203 Denver, Germany). The nanoparticles were placed in a beaker containing 50 mL of distilled water and the beaker was covered to minimize water loss due to evaporation. Each nanoparticle sample was weighed separately; the swelling ratio was calculated using the following equation,

$$\text{swelling ratio} = \frac{W_s - W_d}{W_d} \quad (1)$$

where W_s and W_d are the swollen and dry weights of the nanoparticle samples, respectively.

2.3.6. Deswelling experiments

Retention and release over time of water molecules are the key properties that the swollen nanoparticles must possess if applied for sustained irrigation purposes. To evaluate this property, the water holding potential of nanoparticles was measured by calculating the percent deswelling of the nanocarriers at various time intervals. For this purpose, the nanocarriers were allowed to swell in water until they attained equilibrium, and thereafter left in air to lose water. The deswelling nanoparticles were weighed at specific time intervals and the amount of water lost was calculated. In

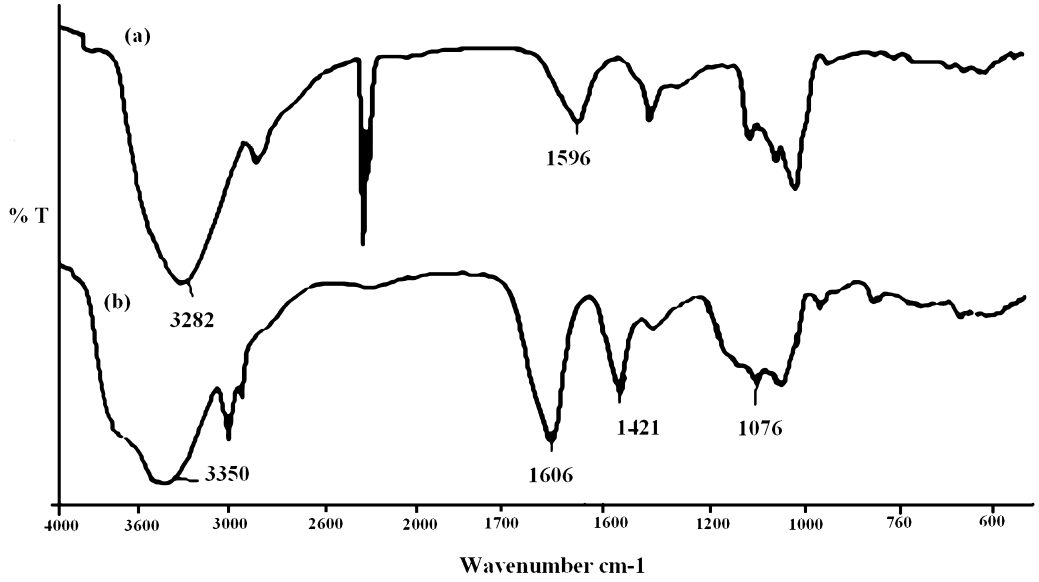

Fig. 1. FTIR spectra of (a) native alginate, and (b) calcium cross-linked alginate nanoparticles.

this way, the percent deswelling of the nanocarriers was calculated using the following equation,

$$\%\ \text{deswelling} = \frac{W_i - W_d}{W_i} \times 100 \quad (2)$$

where W_i and W_d represent the amount of water released at time t and equilibrium, respectively,

2.3.7. Soil pot experiments

To mimic the release experiments performed in agricultural fields, water release studies were performed in a well defined soil-pot system under conditions similar to those prevalent in a common agriculture field. First, soil samples were collected from a two-foot pit making sure that the collected samples were uniform in all respects. After filling each pot with 2 kg of soil, the nanoparticles were added to the pots containing soil and seeds. A separate soil-containing pot was also prepared without nanoparticles as a control. The moisture content of the soil was measured with a digital moisture meter (Mac India Ltd., New Delhi, India) by inserting the instrument sensor into the soil to a specific depth.

2.3.8. Statistical analysis

All experiments were performed at least four times and the data obtained in water absorption and desorption experiments were presented in tables and figures along with their respective standard deviation vales and error bars, respectively.

3. Results and discussion

3.1. FT-IR spectra of calcium alginate nanoparticles

The FTIR spectra of alginate are shown in Fig. 1. It exhibits characteristic peaks of the biopolymer, such as at 3242 cm^{-1} (OH— stretching) (Lawrie et al., 2007), 1596, and 1407 cm^{-1} (COO— asymmetric and symmetric stretching), 1081–1024 cm^{-1} (C—O—C antisymmetric stretching), and carboxyl and carboxylate at about 1000–1400 cm^{-1} (Sankalia et al., 2005). In the spectra of calcium alginate nanoparticles, the asymmetric band of the carboxylate ion has shifted from 1596 cm^{-1} to 1606 cm^{-1}, and the hydroxyl band of sodium alginate has shifted from 3282 cm^{-1} to 3350 cm^{-1}, because of the interaction of sodium alginate and $CaCl_2$ (Lawrie et al., 2007). The appearance of two peaks at 1600 cm^{-1} (asymmetric stretching vibration) and near 1421 cm^{-1} due to symmetric COO— stretching vibration also confirms the presence of alginate.

3.2. XRD spectra of alginate nanoparticles

The XRD spectra of calcium alginate nanoparticles are presented in Fig. 2 and clearly suggest their crystalline nature, mainly due to strong intermolecular hydrogen bonding between alginate chains (Fang, Liu, Jiang, Nie, & Ma, 2011). As is evident from the spectra, the diffraction peaks observed at 13.5, 21.8, and 38.6 degree 2θ may be assigned to the reflection of their (1 1 0) plane from the polyguluronate unit, (2 0 0) plane from the polymannuronate, and others from amorphous halo (Fabia, Slusarczyk, & Gawlowski, 2005). Similar types of diffraction patterns have also been reported elsewhere (Beherei Hanan, El-Magharby, & Abdel-Aal, 2011).

3.3. Zeta potential measurements

The zeta potential of nanoparticles is commonly used to characterize the surface charged properties of nanoparticles (Couvreur, Barratt, Fattal, Legrand, & Vauthier, 2002). The Zetasizer analyzer is based on Photon Correlation Spectroscopy (PCS) or Dynamic Light Scattering (DLS) phenomena, which are used to determine

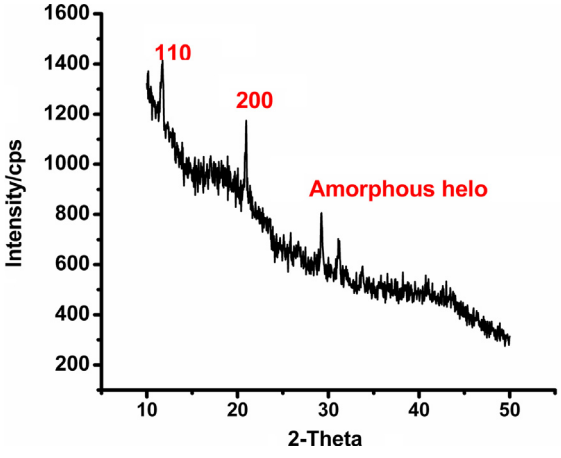

Fig. 2. XRD spectra of alginate nanoparticles.

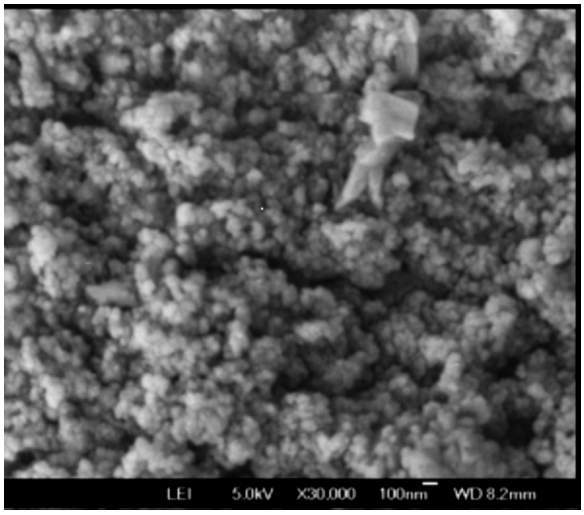

Fig. 3. FESEM image of nanoparticles at 30,000× magnification.

particle size by examining the diffusion rates (*i.e.*, the Brownian motion) of suspended particles. The zeta potential of the nanoparticles was measured and found to be −23.29 mV, which showed that the nanoparticles were anionic in nature. The surface charge also accounts for their fair stability due to electrostatic repulsion.

3.4. Field emission scanning electron microscopy (FESEM)

The swelling and deswelling performance of nanoparticles greatly depend on their size as they directly enhance the surface area of their carriers, resulting in greater contact between the nanoparticles and water molecules or air (in deswelling), as the case may be. Moreover, the morphology of the nanoparticles is another important factor that regulates their water sorption and desorption behavior. The morphological features of prepared nanoparticles were studied by recording their FESEM image as shown in Fig. 3. The image clearly reveals that the size of the nanoparticles varies up to 100 nm and the particles are present as aggregates with cracks on the surfaces. The image also reveals that the alginate particles formed are almost identical in shape.

3.5. Swelling results

3.5.1. Swelling kinetics

The swelling kinetics was investigated to see whether the water sorption process follows first order or second order kinetics. To evaluate the kinetic path of the swelling process, the procedures proposed by Quintana, Valderruten, and Katime (1999) were followed. It is known that for the first order kinetics, the rate of swelling at any time t is directly proportional to the water imbibed by the nanoparticles. The rate of swelling may be expressed as,

$$\frac{dW}{dt} = K(W_\infty - W) \tag{3}$$

where W is the water content of the hydrogel at time t and K is the proportionality constant between the swelling rate and the unrealized swelling capacity $(W_\infty - W)$.

Upon integrating Eq. (3) between the limits $t = 0$ to, t and $W = 0$ to W, the following expression is obtained:

$$ln\frac{W_\infty}{W_\infty - W} = Kt \tag{4}$$

The swelling process of the nanoparticles is considered to follow first order kinetics if the plot of $\ln(W_\infty/W_\infty - W)$ as a function of time yields a straight line. In the present study, the plots obtained

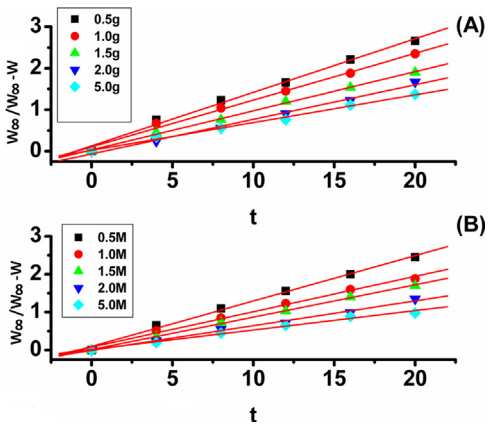

Fig. 4. Plots demonstrating first order kinetic behavior of swelling of nanoparticles with variation in concentrations of (A) calcium chloride, and (B) alginate.

for varying concentrations of calcium chloride and alginate are shown in Fig. 4(A) and (B), respectively, and they confirm the first order kinetic mechanism of the water sorption process.

3.5.2. Effect of alginate

The influence of alginate on the swelling ratio of nanoparticles was investigated by varying the amount of alginate in the feed mixture of nanoparticles in the range from 0.5 to 5.0 g. The results shown in Table 1 indicate that the swelling ratio increases as the quantity of alginate increases up to 1.0 g, while it decreases thereafter as the quantity of alginate continues to increase. The observed initial rise in swelling may be attributed to the increasing hydrophilicity of the nanoparticles, whereas the decrease observed with increasing alginate content may be attributed to the much greater quantity of alginate in the matrix which gives rise to a compact network of biopolymer chains. The greater interaction among alginate macromolecules results in restrained mobility of the network chains. Moreover, a compact structure gives rise to small pore sizes of the network, which also slows down diffusion of water molecules into the particles, thus also bringing about a decrease in the swelling ratio. Similar results have been reported by others (Bajpai & Mishra, 2005).

3.5.3. Effect of a cross-linker

In this study, the effect of cross-linker on the water sorption capacity of nanoparticles was studied by varying the concentration of calcium chloride in a range from 0.5 to 5.0 M. Water sorption data are presented in Table 1 which indicates that the quantity of water imbibed by nanoparticles decreases significantly as the concentration of the cross-linking agent increases. The results are quite obvious as the greater quantity of the cross-linking agent implies the formation of a greater number of smaller size cavities that provide a lower volume to accommodate water molecules thus resulting in lower degree of swelling. Similar results have been reported by other workers (Bajpai & Bhanu, 2004).

3.5.4. Effect of pH

Soil reactivity is often expressed in terms of pH, which is a measure of the acidity or alkalinity of the soil. The pH of soil normally ranges from 3.5 to 9.5, as pH values beyond these extremes are toxic to life (Chang, 1984). Among various factors that influence the water sorption capacity of nanoparticles, the pH is a prime parameter, particularly in those swelling systems in which the water absorbing materials are ionic in nature. In this study, the calcium alginate nanoparticles that possess an anionic charge, along their macromolecules, have been evaluated for their swelling potential. To see their swelling performance with the pH of the swelling

Table 1
Data showing the effect of composition of nanoparticles and temperature and pH of the swelling bath on equilibrium swelling ratio, swelling exponents and diffusion constants.

Sodium alginate (g)	Calcium chloride (M)	Temp. (°C)	pH	Equilibrium swelling ratio	Swelling exponent n	D ($\times 10^{-14}$ cm^2/S)
0.5	0.5	25	7.2	3.20 ± 0.12	0.284	7.85
1.0	0.5	25	7.2	3.85 ± 0.14	0.343	11.5
1.5	0.5	25	7.2	2.90 ± 0.10	0.249	6.10
2.0	0.5	25	7.2	2.64 ± 0.08	0.141	3.10
3.0	0.5	25	7.2	2.12 ± 0.07	0.241	2.68
1.0	1.0	25	7.2	3.23 ± 0.13	0.166	5.39
1.0	1.5	25	7.2	3.01 ± 0.14	0.183	6.55
1.0	2.0	25	7.2	2.58 ± 0.11	0.205	8.2
1.0	3.0	25	7.2	2.20 ± 0.09	0.343	11.5
1.0	5.0	25	7.2	1.68 ± 0.04	0.183	6.55
1.0	0.5	5	7.2	2.22 ± 0.10	0.243	7.34
1.0	0.5	15	7.2	3.40 ± 0.14	0.422	8.21
1.0	0.5	37	7.2	2.90 ± 0.11	0.393	9.64
1.0	0.5	25	4.2	2.95 ± 0.13	0.343	11.5
1.0	0.5	25	9.2	1.65 ± 0.01	0.312	8.8

medium, the pH of the swelling bath was varied in the range from 4.2 to 11. The water sorption data are summarized in Table 1 which indicates that the quantity of water imbibed decreases as the pH increases up to 7.4, while it further decreases when the pH exceeds 7.4. The observed increase in swelling with increasing pH may be explained by the increase in pH of the carboxylic groups present along with the biopolymer chains undergoing ionization thus generating carboxylate anions. These ionic groups produce repulsion forces among anionically charged chains causing them to substantially relax, which in turn permit a greater number of water molecules to enter the alginate network. This clearly results in a greater swelling ratio of nanoparticles. The observed increase in swelling of alginate nanoparticles has also been reported by elsewhere (Foss & Goto, 2004).

From the swelling data shown in Table 1, it can be seen that when the pH exceeds 7.4, the water sorption capacity of nanoparticles decreases drastically. The observed decrease in the degree of swelling may be explained by the fact that, at a much higher alkalinity, the calcium ions tend to bind with the hydroxyl anions, thus breaking bonds with the carboxylate anions of the alginate chains. This results in a collapse of the egg-box structure of the calcium alginate and leads to deswelling of the nanoparticle network.

3.5.5. Effect of temperature

This study was specifically undertaken to judge the suitability of swelling-deswelling nanosystems to see if their water holding and releasing capability may be used to solve irrigation problems arising due to infrequent rainfall in cold desert-like areas. Thus, the role of temperature is quite important and must be evaluated to see how it affects the water sorption behavior of nanoparticles. To study this effect, the temperature of a swelling bath was varied in a range from 5 °C to 37 °C. The swelling data at various temperatures are shown in Table 1, revealing that the swelling ratio increases up to 25 °C, whereas a decrease in the ratio is observed beyond that temperature.

The greater water uptake as the temperature increases may be explained by the fact that, at higher temperatures, the kinetic energy of penetrant water molecules increases as does the relaxing of the alginate chains, collectively leading to significant swelling of the nanoparticles. However, as the temperature rises beyond 25 °C, the swelling ratio decreases, which may be attributed to the weakening of the van der Waal forces operative between the hydrophilic alginate and water molecules. This results in expulsion of water molecules from the bulk of the nanoparticles into the release medium. Some authors (Roy, Bajpai, & Bajpai, 2008) have attributed the observed decrease in water holding capacity to the enhanced tendency of erosion of the alginate nanoparticle layers which brings about a fall in the swelling ratio of the nanoparticles.

3.6. Deswelling study

The water releasing capacity of swollen nanoparticles is an important factor in determining the use of nanoparticles for sustained irrigation in agriculture. Thus, this section describes deswelling behavior of pre-swollen nanoparticles as a function of nanoparticle composition and experimental conditions.

3.6.1. Mechanism of water release

To gain insight into the release mechanisms during deswelling, the following equations, based on Fick's law but applicable to a spherical device, were used (Park, Hempleman, & Propper, 2001):

$$\frac{W_t}{W} Kt^n \tag{5}$$

$$\frac{W_t}{W} = 4\left[\frac{Dt}{\pi r^2}\right] \tag{6}$$

where W_t and W_∞ represent the quantities of water released at time t and equilibrium, respectively, K is the swelling front factor, n is the release exponent, and r is the radius of the dry particles. The value of n determines the nature of the involved release mechanism, *i.e.*, when n is equal to 0.43, the release is Fickian, and when n lies between 0.43 and 0.85, the release mechanism is non-Fickian in nature. Moreover, for n being equal to 0.85, the mechanism is coined as case II, the most desirable condition in controlled release technology. Likewise, the numerical value of the diffusion constant, D, when compared to the numerical value of others also provides information about the internal architecture of the swelling or releasing network.

In this study, the values of n and D for varied concentrations of alginate and calcium chloride are presented in Table 1. The values of n are much smaller than 0.43, whereas those of D do not show a regular trend in their variation.

3.6.2. Effect of alginate

The effect of variation in the amount of alginate on the deswelling behavior of nanoparticles has been studied by varying it in the feed mixture in the range from 0.5 to 5.0 g. The results shown in Fig. 5(a) clearly reveal that the rate of water loss gradually increases with increasing alginate content in the nanoparticles. In other words, by increasing the quantity of biopolymer in the nanoparticles, the tendency of water to loosen gradually increases over time. The observed results may be explained by the fact that

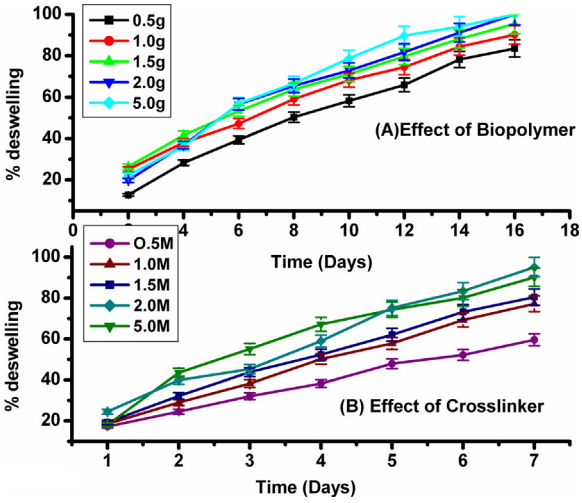

Fig. 5. Effect of variation of % deswelling of water with increasing concentration of (a) alginate, and (b) calcium chloride.

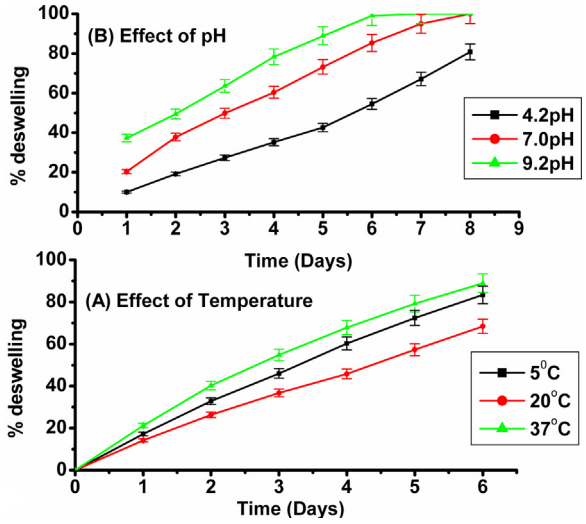

Fig. 6. Effect of (A) temperature, and (B) pH on % deswelling of nanoparticles at fixed chemical composition.

as the alginate content in the nanoparticles increases, the water molecules find more cavities to leave from the bulk of the nanoparticles, thus resulting in greater loss of water. These findings also suggest that for a formulation with long lasting water releasing potential, the alginate content must be kept low. For instance, when alginate content is 0.5 g, only 50 percent of water loss occurs within 15 days, while for nanoparticles with 3.0 g of alginate content almost 90 percent or more of the water is lost in the same time period. Similar deswelling behavior has been reported by other workers (Roy et al., 2008).

3.6.3. Effect of cross-linker

The influence of cross-linker content on the deswelling rate of water was studied by varying the concentration of calcium chloride in a range from 0.5 to 5.0 M. The results are shown in Fig. 5(b) which indicates that the rate of water loss increases with increased concentrations of cross-linker. For example, it is clear from the deswelling profiles that at 0.5 M cross-linker content, water loss is about 80 percent in 15 days, whereas at 2 M concentration, about 100 percent water is lost in the same time period. This obviously suggests that to have a long sustained release of water, the alginate nanoparticles must be cross-linked to a lesser extent. It is also apparent that for nanoparticles cross-linked with 0.5 M calcium chloride, 100 percent water loss requires about 25 days. Thus, depending on the quantity of water needed for a specific time period and crop, the rate of water loss may be controlled as desired. The findings may be attributed to the fact that nanoparticles with a low degree of cross-linking may have wide pores (cavities) that expose a smaller surface area to the atmosphere resulting in a reduced deswelling rate. On the other hand, in greatly cross-linked calcium alginate nanoparticles, cavities of smaller sizes are developed that offer a larger surface area of nanoparticles for deswelling which results in rapid water loss. Similar deswelling behavior has also been reported by other workers (Bajpai, Bajpai, & Mishra, 2006).

3.6.4. Effect of temperature

In this study, the loss in water from deswelling nanoparticles was monitored across a temperature range from 4 °C to 37 °C; the observed deswelling profiles are presented in Fig. 6(a). The results clearly reveal that the water loosening tendency of nanoparticles increases as the atmospheric temperature increases. The figure shows that at 4 °C about 80 percent of the water is lost in 8 days, while at 25 °C; almost 100 percent water is lost over the same time period. When the temperature is increased to 37 °C, 100 percent of the water was lost after only 6 days. Interestingly, these results suggest that in colder regions the swollen nanocarriers may work better, losing water over a longer time than nanocarriers do in hotter areas where the water loosening tendency is enhanced and almost complete water loss occurs in a comparatively shorter time frame. These results are quite expected and may be explained by the fact that with increasing temperature, the water molecules may not be held firmly by the alginate chains, and as a consequence they are lost a little faster. On the other hand, at lower temperatures the binding forces between water molecules and alginate chains remain stronger and therefore water is lost somewhat slower. Alternatively, it is also clear that with increasing temperature the dynamicity of both water molecules and alginate chains is enhanced, which also accounts for a greater rate and quantity of water loss.

3.6.5. Effect of pH

The pH of the soil is an important factor that affects the sustainability of irrigated water. To investigate the influence of soil pH on moisture content, the moisture retention property of the soil mixed with pre-swollen alginate nanoparticles was studied by putting a specific weight of swollen nanoparticles in a predetermined quantity of soil and then periodically determining the moisture content of the soil over time. Specifically, the water released by the nanoparticles was assessed in terms of moisture content at varied pH levels from 4.2 to 11.4. The results are shown in Fig. 6(b), which indicates that at neutral pH of 7.0, the rate of moisture loss is slower than the rate of loss for acidic or basic nature soil. For example, about 65 percent moisture content is retained after 6 days at neutral pH, while more than 80 percent moisture is retained in the same time period. Thus, in the neutral soil, the moisture content due to release of water by the nanoparticles lasts longer than in soils having acidic and basic nature. The observed slower release of water in neutral pH soil may be explained by the fact that due to the poor dissociation of carboxylic groups of alginate, there will be less chain relaxation and, consequently, a lesser quantity of water will be lost to the soil. This situation is very desirable if watering of plants has to be sustained for extended time periods.

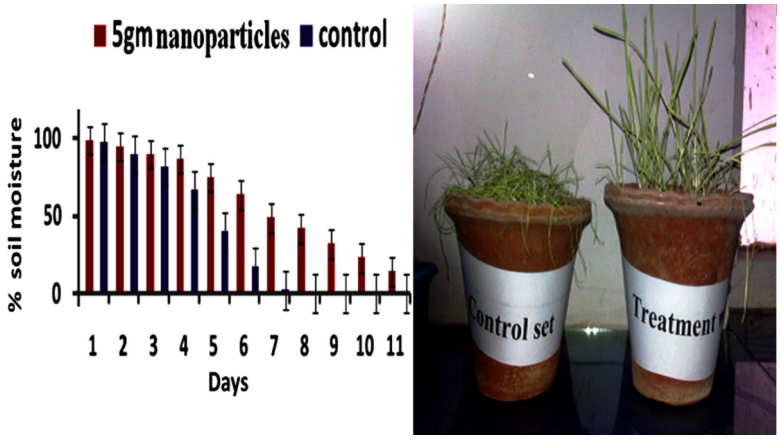

Fig. 7. (Left) Comparative variation of moisture content with time in native soil (control) and nanoparticles mixed soil (5 g NPs with 5 kg soil). (Right) Photograph depicting the difference in plant growth when no nanoparticles are present (left pot) and with nanoparticles (right pot).

3.7. Soil pot experiments

The soil-pot experiments were performed to evaluate the efficiency of the prepared nanoparticles and to see how long they could sustain watering of the plants. The moisture content in the native and nanoparticle-mixed soil at varied time periods is shown in Fig. 7 (left). The results clearly reveal that in native soil the moisture content falls rapidly, whereas in the nanoparticle-mixed soil, the moisture content lasts longer, thus providing a more favorable condition for plant growth. The data show that in the absence of nanoparticles in the soil about 100 percent moisture is lost after 7 days, while for soil mixed with nanoparticles about 20 percent moisture is still retained, even after 11 days. The influence of slow, controlled release of water on plant growth is depicted in Fig. 7 (right), which shows that the plants watered with nanoparticle-mixed soil exhibits better growth. The plants without mixing of nanoparticles stopped growing after the first two weeks and showed signs of dehydration. All the plants in the mixed soil continued to grow for two weeks and were much healthier.

4. Conclusions

Emulsion cross-linking of alginate with calcium ions produces calcium alginate nanoparticles that function as water reservoirs and, therefore, may prove to be an excellent means to provide sustained irrigation in areas where water is scarce. The XRD spectra of nanoparticles prepared in this way show sharp diffraction peaks at 13.5, 21.8, and 38.6, 2θ suggesting for their crystalline nature. The nanoparticles bear a negative potential of 29.3 mV, which imparts stability to their aqueous suspension. The FESEM studies revealed that the particles are nearly identical in size and have a dimension of 100 nm. The nanoparticles exhibit a first order kinetic behavior with respect to variation in the concentration of alginate and cross-linker. When the quantity of alginate in the nanoparticles is increased, the swelling ratio initially increases and thereafter decreases, whereas increasing the quantity of cross-linker results in a significant decrease in water sorption capacity. The extent of water sorption also varies with variation in the pH and temperature of the water reservoir. The water releasing studies suggest that a formulation with less alginate but highly in crosslinked state may be best suited for sustained watering of plants. It was also observed that a soil with neutral pH and a low temperature also favors sustained irrigation. The slow watering potential of nanoparticles was also demonstrated with soil-pot experiments, in which plants exhibited much better growth when nanoparticle-mixed soil was used. Thus, agricultural applications using the developed nanocarriers system may be efficacious for watering plants and fields, especially in those areas where water is scarce or average rainfall quite low.

References

Abd El-Rehirn, H. A., Hegazy, E. S. A., & Abd El-Mohdy, H. L. (2004). Radiation synthesis of hydrogels to enhance sandy soils water retention and increase performance. *Journal of Applied Polymer Science*, *93*, 1360–1371.

Bajpai, J., Bajpai, A. K., & Mishra, S. (2006). Dynamics of controlled release of potassium nitrate from a highly swelling binary biopolymeric blend of alginate and pectin. *Journal of Macromolecular Science. Part A: Pure and Applied Chemistry*, *43*, 1–22.

Bajpai, A. K., & Bhanu, S. (2004). In vitro release dynamics of insulin from a loaded hydrophilic polymeric network. *Journal of Material Science: Materials in Medicine*, *15*, 43–54.

Bajpai, A. K., & Giri, A. (2003). Water sorption behaviour of highly swelling (carboxy methylcellulose-g-polyacrylamide) hydrogels and release of potassium nitrate as agrochemical. *Carbohydrate Polymers*, *53*, 271–279.

Bajpai, A. K., & Mishra, A. (2005). Preparation and characterization of tetracycline-loaded interpenetrating polymers networks of carboxymethyl cellulose and poly (acrylic acid): Water sorption and drug release study. *Polymer International*, *54*, 1347–1356.

Barens, A. R., & Hopfenberg, H. B. (1978). Diffusion and relaxation in glassy polymer powders: 2. Separation of diffusion and relaxation parameters. *Polymer*, *19*, 489–496.

Beherei Hanan, H., El-Magharby, A., & Abdel-Aal, M. S. (2011). Preparation and characterization of novel antibacterial nano-ceramic-composites for bone grafting. *Scholars Research Library Der Pharma Chemica*, *3*(6), 10–27.

Betigeri, S. S., & Neau, S. H. (2002). Immobilization of lipase using hydrophilic polymers in the form of hydrogel beads. *Biomaterials*, *239*(17), 3627–3636.

Bouranis, D. L., Theodoropoulus, A. G., & Drossopoulus, J. B. (1995). Designing synthetic polymers as soil conditioners. *Communications in Soil Science and Plant Analysis*, *26*, 1455–1480.

Buchholz, F. L., & Graham, A. T. (1997). *"Modern superabsorbent polymer technology"*. New York: Wiley.

Buchholz, F. L. (1998). The structure and properties of superabsorbent polyacrylates. In F. L. Buchholz, & A. T. Graham (Eds.), *Modern superabsorbent polymer technology* (pp. 167–221). New York: Wiley-VCH.

Chang, R. (1984). *Chemistry*. Random House, Inc.

Couvreur, P., Barratt, G., Fattal, E., Legrand, P., & Vauthier, C. (2002). Nanocapsule technology: A review. *Critical Reviews™ in Therapeutic Drug Carrier Systems*, *19*, 99–134.

Davis, T. A., Llanes, F., Volesky, B., & Mucci, A. (2003). Metal selectivity of *Sargassum* spp. and their alginates in relation to their L-guluronic acid content and conformation. *Environmental Science & Technology*, *37*, 261–267.

Denuziere, A., Ferrier, D., & Domard, A. (1996). Chitosan-chondroitin sulfate and chitosan-hyaluronate polyelectrolyte complexes. Physio-chemical aspects. *Carbohydrate Polymers*, *29*, 317–323.

Fabia, J., Slusarczyk, C. Z., & Gawlowski, A. (2005). Supermolecular structure of alginate fibres for medical applications studied by means of WAXS and SAXS methods. *Fibres & Textiles in Eastern Europe*, *13*, 114–117.

Fang, D., Liu, Y., Jiang, S., Nie, J., & Ma, G. (2011). Effect of intermolecular intraction on electrospinning of sodium alginate. *Carbohydrate Polymers*, *85*, 276–279.

Foss, A. C., & Goto, T. (2004). Development of acrylic based copolymers for oral insulin delivery. *Pharmaceuticals Biopharmaceuticals*, *57*, 163–169.

George, M., & Abraham, T. E. (2006). Polyionic hydrocolloids for the intestinal delivery of protein drugs: Alginate and chitosan – A review. *Journal of Controlled Release*, *114*, 1–14.

Gombotz, W. R., & Wee, S. F. (1998). Protein release from alginate matrixes. *Advanced Drug Delivery Reviews*, *31*, 267–285.
Gregor, J. E., Fenton, E., Brokenshire, G., Van Den Brink, P., & O'Sullivan, B. (1996). Interactions of calciumand aluminiumions with alginate. *Water Research*, *30*(6), 1319–1324.
Kim, S. R., Yuk, S. H., & John, M. S. (1997). A novel method to enhance the stability of alginate poly-L-lysine-alginate microcapsules. *European Polymer Journal*, *33*, 1009.
Lawrie, G., Keen, I., Drew, B., Chandler-Temple, A., Rintoul, L., Fredericks, P., & Grondahl, L. (2007). Interactions between alginate and chitosan biopolymers characterized using FTIR and XPS. *Biomacromolecules*, *8*, 2533–2541.
Lentz, R. D. (2003). Inhibiting water infiltration with PAM and surfactants: Applications for irrigated agriculture. *Journal of Soil Water Conservation*, *58*, 290–300.
Mararu Carmen, I., Panchapakesan, C. P., Huang, Q., Takhistov, P., Liu, S., & Kokkini, J. L. (2003). Nanotechnology: A new frontier in food science. *Food Technology*, *57*, 24–29.
Oh, J. K., Drumright, R., Siegwart, D. J., & Matyjaszewski, K. (2008). Advanced nanogel engineering for drug delivery. *Progress in Polymer Science*, *33*, 448–477.
Park, D., Hempleman, S. C., & Propper, C. R. (2001). Endosulfan exposure disrupts pheromonal systems in the red-spotted newt: A mechanism for subtle effects of environmental chemicals. *Environmental Health Perspectives*, *109*, 669–673.
Peppas, N. A., Bures, P., Leobandung, W., & Ichikawa, H. (2000). Hydrogels in pharmaceutical formulations. *European Journal of Pharmaceutics and Biopharmaceutics*, *50*(1), 27–46.
Philips, G. O., & Williams, P. A. (Eds.). (2000). *Handbooks of hydrocolloids*. Cambridge: Wood Head Publishing Limited.
Pillay, V., & Fassihi. (1999). In vitro release modulation from crosslinked pellets for site-specific drug delivery to the gastrointestinal tract. II. Physicochemical characterization of calcium-alginate, calcium-pectinate and calcium-alginate-pectinate pellets. *Journal of Controlled Release*, *9*, 243–256.
Quintana, J. R., Valderruten, N. E., & Katime, I. (1999). Synthesis and swelling kinetics of poly(dimethylaminoethyl acrylate methyl chloride quaternary-co-itaconic acid) hydrogels. *Langmuir*, *15*, 4726–4728.
Roy, A., Bajpai, J., & Bajpai, A. K. (2008). Development of calcium alginate-gelatin based microspheres for controlled release of endosulfan as a model pesticide. *Indian Journal of Chemical Technology*, *16*, 388–395.
Saiyed, H., Dewan, A., Bhatnagar, V., Shenoy, U., Shenoy, R., Rajmohan, H., et al. (2003). Effect of endosulfan on male reproductive development. *Environment Health Perspectives*, *111*, 1958–1962.
Sankalia, Mayur G., Mashru, Rajshree C., Sankalia, Jolly M., & Sutariya, Vijay B. (2005). Papain entrapment in alginate beads for stability improvement and site-specific delivery: physicochemical characterization and factorial optimization using neutal network modeling. *AAPS PharmSciTech.*, *6*, 209–222.
Sershen, S., & West, J. (2002). Implantable, polymeric systems for modulated drug delivery. *Advanced Drug Delivery Reviews*, *54*, 1225–1235.
Wang, L., Shelton, R. M., Cooper, P. R., Lawson, M., Triffit, J. T., & Barralet, J. E. (2003). Evaluation of sodium alginate for bone marrow cell tissue engineering. *Biomaterials*, *24*, 3475–3481.
Yeh, P. Y., Kopekova, P., & Kopeek, J. (1994). *Journal of Applied Polymer Science Part A: Chemistry*, *32*, 1627.
Zohuriaan-Mehr, M. J., & Kourosh Kabiri. (2008). Superabsorbent polymer materials: A review. *Iranian Polymer Journal*, *17*(6), 451–477.